Int. J. Solids Structures, 1975, Vol. 11, pp. 213–230. Pergamon Press. Printed in Gt. Britain.

ELASTODYNAMIC BEHAVIOR OF LAMINATED ORTHOTROPIC PLATES UNDER INITIAL STRESS

L. G. BRADFORD and S. B. DONG

Mechanics and Structures Department, School of Engineering and Applied Science, University of California, Los Angeles, California 90024, U.S.A.

(*Received* 7 *January* 1974; *revised* 26 *June* 1974)

Abstract—A finite element method of analysis of the vibrational and wave propagational characteristics is presented for a laminated orthotropic plate under initial stress. The plate may have an arbitrary number of bonded elastic orthotropic layers, each with distinct thickness, density and mechanical properties, and the analysis is capable of treating a completely arbitrary three-dimensional state of initial stress. Biot's theory for incremental elastic deformations of a stressed solid forms the basis for this study. A homogeneous, isotropic plate under two different states of initial stress was analyzed and their numerical results showed excellent correlation with those from an exact solution. Further examples of a three layer composite plate and a sandwich plate are offered to add some general insight to the physical behavior of such plates.

NOTATION

B_{jk}^{lm} quasi-elastic moduli (containing initial stress effect)
C_{jk}^{lm} elastic moduli
C_{jk} contracted notation for elastic moduli, see Appendix.
E_i extensional moduli
Δf_i prescribed incremental surface tractions
G_{jk} shear moduli
H total thickness of plate
$\mathbf{k}$ element stiffness
$\mathbf{k}_g$ element geometrical stiffness
$\mathbf{K}$ plate stiffness
$\mathbf{K}_g$ plate geometrical stiffness
$\mathbf{m}$ element mass
$\mathbf{M}$ plate mass
$\mathbf{r}, \mathbf{r}^*$ arrays of nodal displacement coordinates
$\mathbf{R}$ $\mathbf{R}^T = \{\mathbf{r}^T \mathbf{r}^{*T}\}$, see Equation (21)
S_{ij} components of initial stress
ΔT incremental kinetic energy
u_i rectangular cartesian displacement components
U_j, U_j^* nodal displacement coordinates
$\mathbf{U}$ array of plate nodal displacement coordinates
ΔV incremental potential energy
x_i rectangular cartesian coordinates
δ variational symbol
δ_{ij} Kronecker delta
ϵ_{ij} components of the small strain tensor
λ eigenvalue parameter for elastic stability, see equation (24)
λ_1, λ_2 wave lengths in x_1 and x_2 directions, respectively
ν_{ij} Poisson's ratios
ρ material density
σ_{ij} incremental stress tensor referred to deformed geometry
τ_{ij} incremental stress tensor referred to original geometry
ω_{ij} components of rotation tensor, see equation (2)
ω natural frequency

1. INTRODUCTION

The advantages of multilayered composite materials, which have led to their increased usage, are intuitively apparent and require no elaboration. To design structures composed of such materials, and furthermore, to utilize their inherent characteristics optimally, analytical methods must be available to evaluate their physical behavior.

In this paper the vibrational characteristics of laminated plates under initial stress are considered. It has long been known that a state of initial stress in a body can have a significant influence on its subsequent response to static and dynamic loads. Initial stresses in composites are inevitably present as residual stresses from fabrication processes. Moreover, the possibilities offered by controlled prestressing to effectively exploit the full potential of such materials are exciting and should be of great interest.

Many investigations on vibrations of initially stressed isotropic plates of rectangular and circular planforms based on Kirchhoff theory have been reported and are summarized by Leissa[1]. The extension to orthotropic plates was presented by Lekhnitskii[2]. A finite element analysis of rectangular isotropic plates under arbitrary initial stress states was recently given by Mei and Yang[3]. One of the first comprehensive studies on plates was carried out by Herrmann and Armenàkas[4], who developed a refined theory for initially stressed isotropic plates. Their theory accounted for both transverse shear deformation and rotatory inertia as well as components of initial inplane and transverse shearing stresses. More recently, Sun presented some new analyses of initially stressed isotropic and orthotropic plates and beams[5, 6], which are based on a continuum theory including microstructure. His analyses are primarily intended for laminated structures consisting of two alternating layers, one of which is much stiffer and thicker than the other. The theories and applications in Refs. [1–6] can be grouped as approximate plate theories rather than as a complete three-dimensional model.

The laminated plate considered herein has an arbitrary number of bonded elastic orthotropic layers, each with distinct thickness, density and mechanical properties. The elastic axes of all orthotropic materials coincide with the plate coordinate axes. The analysis is based on Biot's three-dimensional theory for incremental elastic deformations of a stressed solid[7]. It should be pointed out that besides Biot's theory, there is another generally accepted mathematical description of this class of problems due to Trefftz[8]. Bazant[9] concluded from a correlation study of these two theories and variants of them that they were all mutually equivalent. The solution technique employed herein is the Extended Ritz technique, which has been applied to vibrations of laminated plates and cylinders[10–12]. The analysis involves discretization of the plate into a number of subregions termed laminas. A waveform along the propagation direction is explicitly stated at the outset and the dependence through the thickness is treated by a Ritz analysis using suitable interpolation functions within each lamina and appropriate interlaminar continuity conditions. An algebraic eigenvalue problem results from which the modal data can be extracted. Since each lamina is independent, it is possible for it to have not only distinct properties but also a distinct and completely general initial stress state consisting of any or all six components. Thus, it is possible to model completely arbitrary initial stress states, for example one in which the initial stresses may vary over the depth of the plate. Also, the problem of elastic stability of multilayered plates is contained as the special case when the frequency goes to zero. This particular case can also be separately posed as another eigenvalue problem and some comments on this point will be made in the paper.

2. BASIC EQUATIONS FOR AN INITIALLY STRESSED SOLID

Cartesian tensor notation is adopted, and unless otherwise noted, the summation range

implied by a repeated subscript is from 1 to 3. Let the plate have a reference state in which initial stresses S_{jk} are in equilibrium and the material properties relative to this state are assumed known. Equations will be given describing the incremental process which is elastic irrespective of the nature in which the reference state was reached.

In Biot's theory[7], two rectangular Cartesian frameworks are utilized, one denoted by x_j which is fixed with axes running along some suitable directions in the solid and the other in which a local rigid body rotation has occurred. Let u_j be displacement components along the x_j directions. Then, the usual definitions for the components of the small strain and rotation tensors are, respectively:

$$\epsilon_{jk} = \tfrac{1}{2}(u_{j,k} + u_{k,j}) \tag{1}$$

$$\omega_{jk} = \tfrac{1}{2}(u_{j,k} - u_{k,j}). \tag{2}$$

The constitutive relation for the incremental stresses and strains can be cast into two alternate but equivalent forms:

$$\tau_{jk} = C^{lm}_{jk}\epsilon_{lm} \tag{3}$$

or

$$\sigma_{jk} = B^{lm}_{jk}\epsilon_{lm}. \tag{4}$$

In equations (3) and (4), τ_{jk} and σ_{jk} are incremental stress components in the rotated coordinate system referred to unit area before and after deformation, respectively. The transformation between τ_{jk} and σ_{jk} is given by:

$$\tau_{jk} = \sigma_{jk} + S_{ik}\epsilon_{il} - \tfrac{1}{2}(S_{jl}\epsilon_{lk} + S_{kl}\epsilon_{jl}). \tag{5}$$

The C^{lm}_{jk} in (3) are the usual elastic coefficients which have symmetry about their indices and can be regarded as the dual of those in the constitutive law for an unstressed solid, except now they are referred to the present reference state. The B^{lm}_{jk} are quasi elastic coefficients, and in general they are not symmetric about their indices due to initial stresses S_{jk}. The relation between C^{lm}_{jk} and B^{lm}_{jk} is:

$$B^{lm}_{jk} = C^{lm}_{jk} - S_{jk}\delta_{lm} + \tfrac{1}{4}(S_{jm}\delta_{lk} + S_{jl}\delta_{mk} + S_{km}\delta_{lj} + S_{kl}\delta_{mj}) \tag{6}$$

where δ_{jk} is the Kronecker symbol. For an orthotropic solid, the explicit form of (6) in matrix notation is:

$$[B^{lm}_{jk}] = \begin{bmatrix} C^{11}_{11} & C^{22}_{11} & C^{33}_{11} & 0 & 0 & 0 \\ & C^{22}_{22} & C^{33}_{22} & 0 & 0 & 0 \\ & & C^{33}_{33} & 0 & 0 & 0 \\ & & & C^{23}_{23} & 0 & 0 \\ & & & & C^{13}_{13} & 0 \\ & & & & & C^{12}_{12} \end{bmatrix} + \begin{bmatrix} 0 & -S_{11} & -S_{11} & 0 & S_{13}/2 & S_{12}/2 \\ -S_{22} & 0 & -S_{22} & S_{23}/2 & 0 & S_{12}/2 \\ -S_{33} & -S_{33} & 0 & S_{23}/2 & S_{13}/2 & 0 \\ -S_{23} & -S_{23}/2 & -S_{23}/2 & (S_{22}+S_{33})/4 & S_{12}/4 & S_{13}/4 \\ -S_{13}/2 & -S_{13} & -S_{13}/2 & S_{12}/4 & (S_{11}+S_{33})/4 & S_{23}/4 \\ -S_{12}/2 & -S_{12}/2 & -S_{12} & S_{13}/4 & S_{23}/4 & (S_{11}+S_{22})/4 \end{bmatrix} \tag{7}$$

It can be seen from (7) that even though the material is orthotropic, constitutive relation (4) appears to be more general than that for orthotropy because of what can be called "stress-induced" anisotropy.

The stress equations of motion and the associated traction boundary conditions for a stressed solid are:

$$(\tau_{jk} + S_{jk} + S_{lk}\omega_{jl} + \tfrac{1}{2}S_{lk}\epsilon_{lj} - \tfrac{1}{2}S_{lj}\epsilon_{lk})_{,k} = \rho\ddot{u}_j \tag{8}$$

$$(\tau_{jk} + S_{lk}\omega_{jl} + \tfrac{1}{2}S_{lk}\epsilon_{lj} - \tfrac{1}{2}S_{lj}\epsilon_{lk})n_k = \Delta f_j \tag{9}$$

where n_k are the components of the outward unit normal, ρ is the density and Δf_j are the prescribed incremental surface tractions.

The variational principle leading to equations of motion (8) and boundary conditions (9) can be stated as:

$$\delta(\Delta V - \Delta T) - \int_{surf}\int \Delta f_j \delta u_j \, ds = 0 \tag{10}$$

where ΔT and ΔV are the incremental kinetic and strain energies and have the forms:

$$\Delta T = \int_{Vol}\int\int \frac{1}{2}\rho\dot{u}_l\dot{u}_l \, dvol \tag{11}$$

$$\Delta V = \Delta V_1 + \Delta V_2 \tag{12}$$

with

$$\Delta V_1 = \int_{Vol}\int\int \frac{1}{2}\tau_{jk}\epsilon_{jk} \, dvol = \int_{Vol}\int\int \frac{1}{2}C_{jk}^{lm}\epsilon_{lm}\epsilon_{jk} \, dvol \tag{12a}$$

$$\Delta V_2 = \int_{Vol}\int\int \frac{1}{2}S_{jk}(\epsilon_{jl}\omega_{lk} + \epsilon_{kl}\omega_{lj} + \omega_{jl}\omega_{kl}) \, dvol. \tag{12b}$$

The breakdown of ΔV into ΔV_1 and ΔV_2 is for convenience only. Note that ΔV_1 has exactly the same form as that for an unstressed solid and it is associated with the strain energy due to incremental stresses only. The other part ΔV_2 accounts for the strain energy due to the presence of initial stresses during the incremental deformation process. It will be seen in the next section on the formulation of the analysis and solution technique that ΔV_1 leads to the usual stiffness matrix while ΔV_2 gives rise to an initial stress or geometrical stiffness matrix.

3. EXTENDED RITZ ANALYSIS OF A PLATE

Consider a plate composed of an arbitrary number of bonded elastic orthotropic layers. Let Cartesian coordinates x_j be established with x_1, x_2 in the plane of the plate and x_3 normal to it. The orthotropy axes for all layers coincide with the x_j coordinate directions. In an Extended Ritz analysis, the plate is discretized into a number of laminas, each of which may have distinct properties, thickness and initial stress state.

The displacement field within a lamina can be taken as:

$$\begin{aligned} u_j(x_k, t) &= \{U_j(x_3) + iU_j^*(x_3)\}\, e^{i(\omega t + \xi x_1 + \eta x_2)} \qquad (j = 1, 2) \\ u_3(x_k, t) &= \{iU_3(x_3) + U_3^*(x_3)\}\, e^{i(\omega t + \xi x_1 + \eta x_2)} \end{aligned} \tag{13}$$

where ω is the natural frequency and $\xi = \pi/\lambda_1$, $\eta = \pi/\lambda_2$ are wave numbers along x_1, x_2, respectively. It can be seen from (13) that the dependence of the waveform is explicit along the propagation direction, but is as yet undetermined in x_3 of the plate. The functions U_i (and U_j^*) can be approximated by a quadratic interpolation:

$$U_j(x_3) = U_{jb}(1-3x+2x^2) + U_{jm}(4x-4x^2) + U_{jf}(2x^2-x) \tag{14}$$

where

$$x = (x_3 - x_{3b})/(x_{3f} - x_{3b}) \tag{15}$$

and x_{3b}, x_{3f} are the thickness coordinates of the bounding surfaces of the lamina. The generalized coordinates U_{jb}, U_{jm}, U_{jf} (and U_{jb}^*, U_{jm}^*, U_{jf}^*) represent the values of the U_j (and U_j^*) displacement at the back, mid and front nodal surfaces. It was found in Refs. [10–12] that a suitable number of these elements with quadratic interpolation (14) possess excellent modelling capability of the physical phenomena over a wide range of frequencies and wave lengths. The imaginary unit i (corresponding to $i = e^{i\pi/2}$) provides for a $\pi/2$ phase difference between those displacements with and without it. The necessity of including U_j^* arises because of initial stress components S_{13}, S_{23} and they cause coupling of U_j with U_j^*. In the case when S_{13}, S_{23} are absent, then it is possible to consider only one wave form, U_j, or U_j^*, as both will represent identical waves that are separated by a $\pi/2$ phase shift. This will be clearly seen in the derivation of the stiffness matrix.

It is noted that wave form (13) can be taken to represent a propagating plane wave whose wave length is the vectorial sum of the wave lengths along x_1 and x_2, i.e. $\simeq\{(\pi/\xi)^2 + (\pi/\eta)^2\}^{1/2}$. Thus, it is possible to reduce the number of independent spatial variables by one for the analysis. However, in so doing, the orthotropic properties must undergo a corresponding rotational transformation to the propagation direction and this leads to a constitutive relation that appears to have an anisotropic form more general than orthotropy, even though the fact remains that only nine of the elastic coefficients are independent. To avoid this difficulty, it is more convenient to treat the displacement field in terms of a pair of superposed orthogonal waves.

The lamina potential and kinetic energies can be obtained by using (12) and (11). However, because complex displacements (13) are involved, it is necessary to modify the forms of (11) and (12) by using complex conjugate quantities so that real energies are possible. It is possible to cast the expressions for ΔV_1, ΔV_2 and ΔT entirely in terms of displacements by substituting (1) and (2) into (11) and (12). Thus

$$\begin{aligned}\Delta V_1 = \frac{1}{2}\int\int_{Vol}\int \{&C_{11}^{11}u_{1,1}\bar{u}_{1,1} + C_{22}^{22}u_{2,2}\bar{u}_{2,2} + C_{33}^{33}u_{3,3}\bar{u}_{3,3} \\ &+ C_{22}^{33}(u_{2,2}\bar{u}_{3,3} + \bar{u}_{2,2}u_{3,3}) + C_{11}^{33}(u_{3,3}\bar{u}_{1,1} + \bar{u}_{3,3}u_{1,1}) + C_{11}^{22}(u_{1,1}\bar{u}_{2,2} + \bar{u}_{1,1}u_{2,2}) \\ &+ C_{23}^{23}(u_{2,3}\bar{u}_{2,3} + u_{2,3}\bar{u}_{3,2} + \bar{u}_{2,3}u_{3,2} + u_{3,2}\bar{u}_{3,2}) + C_{13}^{13}(u_{3,1}\bar{u}_{3,1} + u_{3,1}\bar{u}_{1,3} + \bar{u}_{3,1}u_{1,3} + u_{1,3}\bar{u}_{1,3}) \\ &+ C_{12}^{12}(u_{1,2}\bar{u}_{1,2} + u_{1,2}\bar{u}_{2,1} + \bar{u}_{1,2}u_{2,1} + u_{2,1}\bar{u}_{2,1})\}\,dx_1\,dx_2\,dx_3\end{aligned} \tag{16}$$

$$\begin{aligned}\Delta V_2 = \frac{1}{2}\int\int_{Vol}\int \frac{1}{4}\{&S_{11}(3u_{2,1}\bar{u}_{2,1} - u_{1,2}\bar{u}_{1,2} + 3u_{3,1}\bar{u}_{3,1} - u_{1,3}\bar{u}_{1,3} - u_{1,2}\bar{u}_{2,1} - \bar{u}_{1,2}u_{2,1} - u_{1,3}\bar{u}_{3,1} - \bar{u}_{1,3}u_{3,1}) \\ &+ S_{22}(3u_{1,2}\bar{u}_{1,2} - u_{2,1}\bar{u}_{2,1} + 3u_{3,2}\bar{u}_{3,2} - u_{2,3}\bar{u}_{2,3} - u_{2,1}\bar{u}_{1,2} - \bar{u}_{2,1}u_{1,2} - u_{2,3}\bar{u}_{3,2} - \bar{u}_{2,3}u_{3,2})\end{aligned}$$

$$+ S_{33}(3u_{1,3}\bar{u}_{1,3} - u_{3,1}\bar{u}_{3,1} + 3u_{2,3}\bar{u}_{2,3} - u_{3,2}\bar{u}_{3,2} - u_{3,1}\bar{u}_{1,3} - \bar{u}_{3,1}u_{1,3} - u_{3,2}\bar{u}_{2,3} - \bar{u}_{3,2}u_{2,3})$$
$$+ S_{12}(2u_{1,1}\bar{u}_{1,2} + 2\bar{u}_{1,1}u_{1,2} - 2u_{1,1}\bar{u}_{2,1} - 2\bar{u}_{1,1}u_{2,1} + 2u_{2,2}\bar{u}_{2,1} + 2\bar{u}_{2,2}u_{2,1} - 2u_{2,2}\bar{u}_{1,2} - 2\bar{u}_{2,2}u_{1,2}$$
$$+ 3u_{3,1}\bar{u}_{3,2} + 3\bar{u}_{3,1}u_{3,2} - u_{1,3}\bar{u}_{2,3} - \bar{u}_{1,3}u_{2,3} - u_{1,3}\bar{u}_{3,2} - \bar{u}_{1,3}u_{3,2} - u_{3,1}\bar{u}_{2,3} - \bar{u}_{3,1}u_{2,3})$$
$$+ S_{23}(2u_{2,2}\bar{u}_{2,3} + 2\bar{u}_{2,2}u_{2,3} - 2u_{2,2}\bar{u}_{3,2} - 2\bar{u}_{2,2}u_{3,2} + 2u_{3,3}\bar{u}_{3,2} + 2\bar{u}_{3,3}u_{3,2} - 2u_{3,3}\bar{u}_{2,3} - 2\bar{u}_{3,3}u_{2,3}$$
$$+ 3u_{1,2}\bar{u}_{1,3} + 3\bar{u}_{1,2}u_{1,3} - u_{2,1}\bar{u}_{3,1} - \bar{u}_{2,1}u_{3,1} - u_{2,1}\bar{u}_{1,3} - \bar{u}_{2,1}u_{1,3} - u_{1,2}\bar{u}_{3,1} - \bar{u}_{1,2}u_{3,1}) \tag{17}$$
$$+ S_{13}(2u_{1,1}\bar{u}_{1,3} + 2\bar{u}_{1,1}u_{1,3} - 2u_{1,1}\bar{u}_{3,1} - 2\bar{u}_{1,1}u_{3,1} + 2u_{3,3}\bar{u}_{3,1} + 2\bar{u}_{3,3}u_{3,1} - 2u_{3,3}\bar{u}_{1,3} - 2\bar{u}_{3,3}u_{1,3}$$
$$+ 3u_{2,1}\bar{u}_{2,3} + 3\bar{u}_{2,1}u_{2,3} - u_{1,2}\bar{u}_{3,2} - \bar{u}_{1,2}u_{3,2} - u_{1,2}\bar{u}_{2,3} - \bar{u}_{1,2}u_{2,3} - u_{2,1}\bar{u}_{3,2} - \bar{u}_{2,1}u_{3,2})\} \, dx_1 \, dx_2 \, dx_3$$

$$\Delta T = \frac{1}{2}\int\int\int_{Vol} \rho\{\dot{u}_1\bar{\dot{u}}_1 + \dot{u}_2\bar{\dot{u}}_2 + \dot{u}_3\bar{\dot{u}}_3\} \, dx_1 \, dx_2 \, dx_3 \tag{18}$$

where the superior bars indicate complex conjugation. Substituting displacement form (13) into (16), (17) and (18) and observing that the limits of integration over the depth of the lamina is (x_{3b}, x_{3f}), there results integrals with integrands of the form:

$$\Delta V_1 = \int\int dx_1 \, dx_2 \int_{x_{3b}}^{x_{3f}} f(x_3, C_{jk}^{lm}, \xi, \eta, U_{nb}, U_{nm}, \ldots U_{nf}^*) \, dx_3 \tag{16a}$$

$$\Delta V_2 = \int\int dx_1 \, dx_2 \int_{x_{3b}}^{x_{3f}} f(x_3, S_{jk}, \xi, \eta, U_{nb}, U_{nm}, \ldots U_{nf}^*) \, dx_3 \tag{17a}$$

$$\Delta T = -\omega^2 \int\int dx_1 \, dx_2 \int_{x_{3b}}^{x_{3f}} f(x_3, U_{nb}, U_{nm}, U_{nf}, U_{nb}^*, U_{nm}^*, U_{nf}^*) \, dx_3. \tag{18a}$$

Three important features should be noted. First, it is seen that the integrands in (16a, 17a, 18a) are not functions of x_1 and x_2 and that the corresponding double integral is the same for all three expressions. Hence they can be removed from consideration in this problem when the variational principle (10) is applied. Secondly, it can be seen that ΔV_1, which is associated with the strain energy of the incremental stresses only, will lead to contributions in the total element stiffness matrix which are the same as that for an unstressed solid[12, 10]. Lastly, recall that because constitutive relation (4) was not symmetric due particularly to the initial stresses S_{jk}, it was not obvious at the outset that ΔV_2 would lead to contributions for the total element stiffness matrix that are symmetric about its principal diagonal. However, by examining (17), it is clear that ΔV_2, which is associated with initial stress or geometrical stiffness matrix contributions, will in fact possess symmetry. Thus, the total element stiffness matrix will be symmetric, and unless the initial stresses exceed those limits causing instability, it will be positive definite so that real frequencies can be expected.

Carrying out the integrations indicated in (16a), (17a), (18a) leads to results for ΔV and ΔT of the form

$$\Delta V = \tfrac{1}{2}\mathbf{R}^T[\mathbf{k} + \mathbf{k}_g]\mathbf{R} \tag{19}$$

$$\Delta T = -\tfrac{1}{2}\omega^2\mathbf{R}^T\mathbf{m}\mathbf{R} \tag{20}$$

where

$$\mathbf{R}^T = \{\mathbf{r}^T\mathbf{r}^{*T}\} \tag{21}$$

and

$$\mathbf{r}^T = \{U_{1b}, U_{2b}, U_{3b}, U_{1m}, U_{2m}, U_{3m}, U_{1f}, U_{2f}, U_{3f}\} \tag{21a}$$

$$\mathbf{r}^{*T} = \{U_{1b}^*, U_{2b}^*, U_{3b}^*, U_{1m}^*, U_{2m}^*, U_{3m}^*, U_{1f}^*, U_{2f}^*, U_{3f}^*\}. \tag{21b}$$

The element stiffness $\mathbf{k}$, geometrical stiffness $\mathbf{k}_g$ and $\mathbf{m}$ matrices in (19) and (20) are of rank 18×18 and can be partitioned into following matrices, each of which has a rank of 9×9.

$$\mathbf{k} = \begin{bmatrix} \mathbf{k}_1 & 0 \\ 0 & \mathbf{k}_1 \end{bmatrix}; \qquad \mathbf{k}_g = \begin{bmatrix} \mathbf{k}_2 & \mathbf{k}_3 \\ \mathbf{k}_3{}^T & \mathbf{k}_2 \end{bmatrix}; \qquad \mathbf{m} = \begin{bmatrix} \mathbf{m}_1 & 0 \\ 0 & \mathbf{m}_1 \end{bmatrix}. \tag{22}$$

The explicit forms of $\mathbf{k}_1$, $\mathbf{k}_2$, $\mathbf{k}_3$ and $\mathbf{m}_1$ are given in the Appendix. It can be seen (19), (21) and (22) that $\mathbf{r}$ and $\mathbf{r}^*$ are coupled through the submatrix $\mathbf{k}_3$ given in the Appendix, it can be seen that this coupling is due to the presence of S_{13} and S_{23}, the initial transverse shear stresses. If these initial stress components are absent, then it is possible to consider only one waveform consisting of only one set of generalized coordinates, either $\mathbf{r}$ or $\mathbf{r}^*$, as identical stiffness and mass matrices will be encountered. Recall that these two waveforms are identical and are separated by a $\pi/2$ phase difference as seen in (13).

Variation of the sum of all lamina potential and kinetic energies comprising the plate results in the following algebraic eigenvalue problem.

$$[\mathbf{K} + \mathbf{K}_G]\mathbf{U} = \omega^2 \mathbf{M}\mathbf{U} \tag{23}$$

where $\mathbf{U}$ is an ordered set of generalized coordinates for the plate and contains $\mathbf{r}$ only for each element or both $\mathbf{r}$ and $\mathbf{r}^*$ depending on the nature of the initial stress state. In (23), $\mathbf{K}$, $\mathbf{K}_G$ and $\mathbf{M}$ are, respectively, the plate stiffness, geometrical stiffness and mass matrices.

Equation (23) is solved by means of a direct-iterative eigensolution technique described in Refs. [14, 15]. The essence of this method is a reduction of the rank of the algebraic eigensystem with a suitably chosen set of reduced generalized coordinates. The eigenvalue problem is solved in this reduced space. This process is iterated until convergence of the results has been reached. Its convergence is assured because the method is akin to the Stodola–Vianello technique except that it is applied to a group of eigenvectors simultaneously instead of only one. The method is extremely efficient computationally. For this paper, the computer code was written using 16 vectors for the reduced space and iteration was performed until the lowest ten converged within a preset tolerance.

4. A NOTE ON ELASTIC STABILITY ANALYSIS

The elastic stability of a multilayered plate for a given set of wave numbers, ξ, η is said to occur if the corresponding frequency goes to zero. It is also possible to treat this problem separately. In (23), let $\omega^2 = 0$ and introduce a parameter λ such that

$$[\mathbf{K} + \lambda \mathbf{K}_G]\mathbf{U} = 0. \tag{24}$$

The parameter λ has the meaning as the ratio of the critical initial stress state to the present initial stress state. Thus, an alternate eigenvalue problem (24) results for the determination of the lowest critical absolute value of λ. The concept of reducing the rank of the eigenvalue problem can also be applied here [13], and the direct-iterative eigensolution technique [14, 15] can again be used.

5. HOMOGENEOUS, ISOTROPIC PLATE

In this set of calculations, an opportunity was provided to verify the computer code and determine the accuracy of the modeling technique. Numerical results were compared with those based on analytical methods. In addition, data were generated to illustrate the physical behavior of homogeneous, isotropic plates under various states of initial stress.

A plate with unit thickness ($H = 1$) and Poisson's ratio $\nu = 0{\cdot}3$ was adopted and it was modeled with 20 equal size laminas. This corresponded to 41 nodal planes and the number of degrees of freedom ranged from 82 to 246 depending on the nature of the initial stress and the propagation direction. Stress free surface conditions were prescribed. All quoted frequencies are normalized with respect to the third lowest frequency at cutoff for that of an unstressed plate, i.e.

$$\omega_{ref} = (\pi/h)\sqrt{G/\rho} \tag{25}$$

where G and ρ are the shear modulus and unit density, respectively. The values of initial stress are normalized with respect to G, i.e. $\bar{S}_{ij} = S_{ij}/G$.

Frequencies at selected wave numbers for a plate under (1) uniform tension, (2) uniform in-plane shear, and (3) uniform transverse shear are presented in Tables 1, 2, 3, respectively. Also shown in these tables are results obtained by analytical techniques, such as by an established frequency equation ((Biot[7] pp. 327–328) Table 1) or by a regula falsi procedure applied to the equations of motion and the prescribed boundary conditions (Tables 2, 3). Examination of these results shows extremely good agreement for the range of thickness modes and for all of the initial stress states considered.

In Fig. 1, frequency spectra for the lowest four plane wave modes are plotted with the magnitude of the uniform tension as a parameter. As noted the initial stress $\bar{S}_{11}$ is a normalized value taken with respect to G, so that some of the values may appear to be unrealistically high. These values were contrived only for purposes of showing sufficient differences in the frequencies in the range of wave numbers considered. It can be seen that only the lowest mode is affected over the entire wave number range by the initial stress. In the other three modes, the effect is not pronouncedly felt until the higher wave numbers.

In Fig. 2, the lowest two plane wave modes are plotted for a flexural-type initial stress state. The exact initial stress distribution as illustrated in this figure, actually consisted of a stepwise series of constant initial stress in each of the laminas. Displacement patterns for these two modes at $H/\lambda_1 = 1{\cdot}0$ are shown in Fig. 3.

Table 1. Normalized natural frequencies—homogeneous isotropic plate under uniform axial stress

	$H/\lambda_1 = 0{\cdot}10$		$H/\lambda_1 = 0{\cdot}0$		$H/\lambda_1 = 1{\cdot}0$		$H/\lambda_1 = 0{\cdot}0$	
	$\bar{S}_{11} = 0{\cdot}005$		$\bar{S}_{11} = -0{\cdot}005$		$\bar{S}_{11} = 0.25$		$\bar{S}_{11} = -0{\cdot}25$	
Mode	Computed†	Anal‡	Computed†	Anal‡	Computed†	Anal‡	Computed†	Anal‡
1	0·016634	0·016633	0·013322	0·013321	0·898450	0·898447	0·626318	0·626317
2	0·168902	0·168902	0·168902	0·168902	1·456109	1·456109	1·367616	1·367615
3	1·016327	1·016326	1·017562	1·017562	1·899735	1·899732	1·914167	1·914164
4	1·849655	1·849653	1·849909	1·849907	2·010411	2·010406	1·991742	1·991737
5	2·027708	2·027696	2·029918	2·029906	2·796982	2·796959	2·855243	2·855218
6	2·997824	2·997723	3·001536	3·001435	3·036039	3·035947	3·112899	3·112807
7	3·747113	3·747087	3·747133	3·747107	4·033863	4·033437	4·191346	4·191234
8	3·998996	3·998572	4·003981	4·003556	4·155283	4·155166	4·217212	4·216762

†82 degrees of freedom.
‡Biot's frequency equation (Ref. [7] pp. 327–328).

Table 2. Normalized natural frequencies—homogeneous, isotropic plate under uniform in-plane shear

	$H/\lambda_1 = 0{\cdot}30$	$H/\lambda_2 = 0{\cdot}30$
	$\bar{\bar{S}}_{12} = 0{\cdot}25$	
Mode	Computed†	Anal‡
1	0·938459	0·938459
2	1·490188	1·490188
3	2·220716	2·220715
4	3·564705	3·564704
5	3·849546	3·849543
6	5·471525	5·471508
7	6·988052	6·988019
8	9·162458	9·162155
9	12·02694	12·02682
10	12·25184	12·25054

†123 degrees of freedom.
‡By regula falsi.

Table 3. Normalized natural frequencies—homogeneous, isotropic plate under uniform transverse shear

	$H/\lambda_1 = 0{\cdot}30$,	$H/\lambda_2 = 0{\cdot}0$
	$\bar{\bar{S}}_{13} = 0{\cdot}25$	
Mode	Computed†	Anal‡
1	0·303722	0·303722
2	0·925763	0·925762
3	1·584650	1·584649
4	3·275156	3·275155
5	3·552424	3·552422

†246 degrees of freedom.
‡By regula falsi.

Before proceeding to another example, a brief mention of one calculation on the elastic stability limit of a thin isotropic plate is made. Using the same model through the thickness (20 elements) for a square plate ($H/\lambda_1 = H/\lambda_2 = 0{\cdot}01$), the computed critical uni-directional stress $\bar{\bar{S}}_{11}$ for buckling was $\bar{\bar{S}}_{11} = -9{\cdot}39445 \times 10^{-4}$. That obtained from classical plate theory (Timoshenko and Gere [16]) was $\bar{\bar{S}}_{11} = \sigma_{cr}/G = -9{\cdot}39962 \times 10^{-4}$ where $\sigma_{cr} = [-kE/12(1-\nu^2)] \times (\pi H/\lambda)^2$ with $k = 4$. Thus, both results are in good agreement of each other.

6. COMPOSITE PLATE

Frequency analyses were conducted on a laminated plate composed of three layers, all of the same material (a high modulus fiber-reinforced composite) but oriented in different directions. The properties of this composite are:

$$E_L/E_T = 25, \quad G_{LT}/E_T = 0{\cdot}5, \quad G_{TT}/E_T = 0{\cdot}2, \quad \nu_{LT} = 0{\cdot}25 \tag{26}$$

where L and T are directions parallel and transverse to the fibers, respectively. For the present

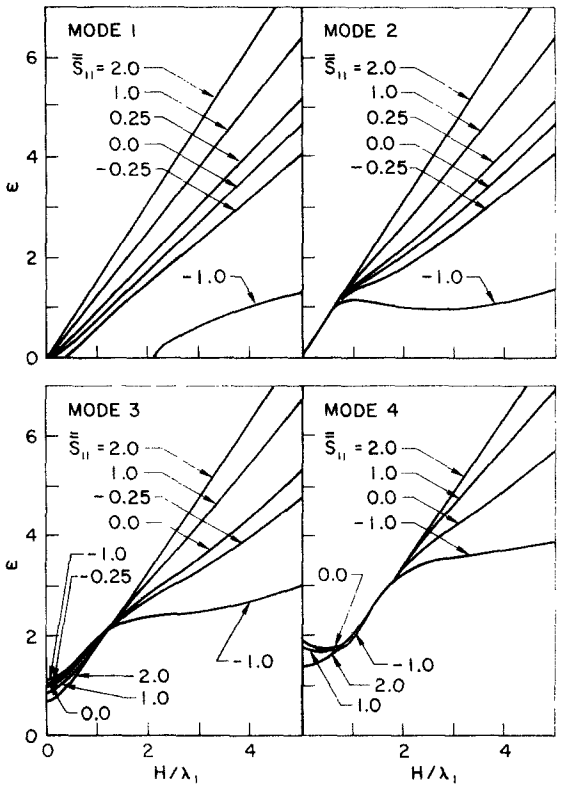

Fig. 1. Frequency spectra for lowest four plane wave modes under initial uniform tension $\bar{\bar{S}}_{11} = S_{11}/G$.

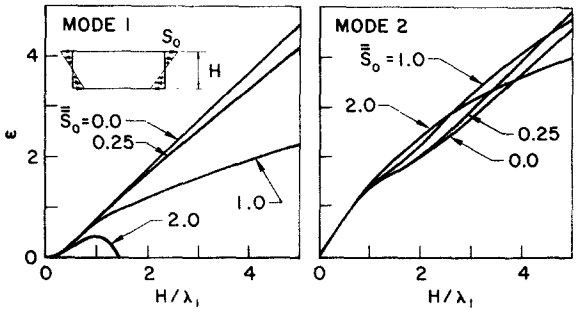

Fig. 2. Frequency spectra for lowest two plane wave modes under initial flexural stress distribution $\bar{\bar{S}}_0 = S_0/G$.

analysis, both E_T and ρ the material density, can be set equal to unity without loss of generality. The coefficients C_{ij} corresponding to (26) with fibers oriented along the x_1 direction are:

$$C_{ij} = \begin{bmatrix} 25{\cdot}17 & 0{\cdot}3356 & 0{\cdot}3356 & & & \\ & 1{\cdot}0710 & 0{\cdot}2711 & & & \\ & & 1{\cdot}0710 & & & \\ & & & 0{\cdot}2 & & \\ & & & & 0{\cdot}5 & \\ & & & & & 0{\cdot}5 \end{bmatrix} \tag{26a}$$

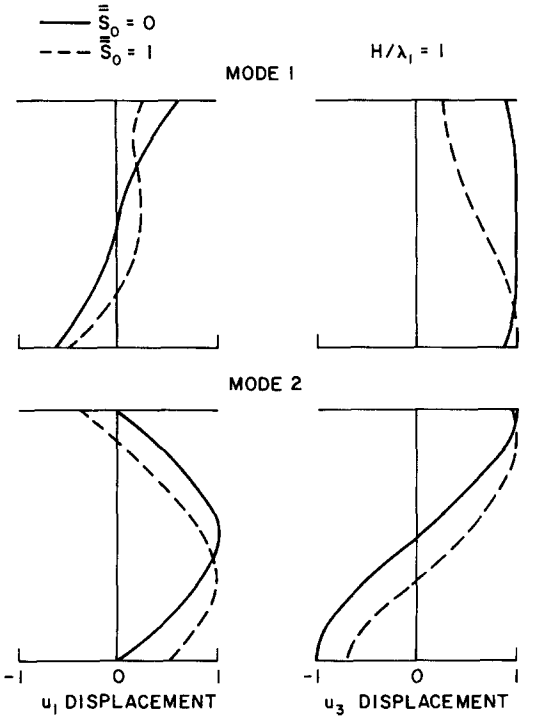

Fig. 3. Displacement distribution for lowest two plane wave modes under initial flexural stress distribution.

a $\pi/2$ rotation of (26a) about the x_3 axis gives the appropriate values of C_{ij} for fibers along the x_2 direction. The laminate construction is 0°–90°–0° cross-ply as shown in Fig. 4 and thicknesses of the outer laminates are $0{\cdot}3H$ and $0{\cdot}2H$ and the middle laminate is $0{\cdot}5H$, where H is the total plate thickness. A model was adopted consisting of 20 equal-thickness elements corresponding to 41 nodal surfaces. The exact number of degres of freedom depends, of course, on the nature of the initial stress state. For the two cases of initial stress states considered for the square plate ($\xi = \eta$), (1) uniform axial stress in both directions ($S_{11} = S_{22}$) and (2) uniform transverse shears in both directions ($S_{13} = S_{23}$), 123 and 246 degrees of freedom, respectively, were required. Stress free surface conditions were prescribed. In these problems, S_{ij} is normalized according to $S_{ij} = S_{ij}/E_T$.

In Fig. 4, the lowest modes of a square plate are plotted for an initial stress of uniform axial stress in both directions. As can be seen, the most significant frequency variations occur in the lowest mode. The typical increase in frequency due to intial tension and decrease due to initial compression until instability are again evident. Effects upon the higher modes are not pronounced until the larger wave numbers, a phenomenon which has been seen in the previous isotropic plate analysis.

In Fig. 5 the lowest four modes of the same plate under the uniform transverse shear stress state ($S_{13} = S_{23}$) are plotted. In all four modes, this initial stress state causes a decrease in frequency for the wave number range considered. In the lowest mode, it can be seen that instabilities are possible, especially at particularly small wave numbers.

7. SANDWICH PLATE

Sandwich construction is a special class of laminated structures which has been extensively employed. Furthermore, there have been some interest in achieving optimum design by

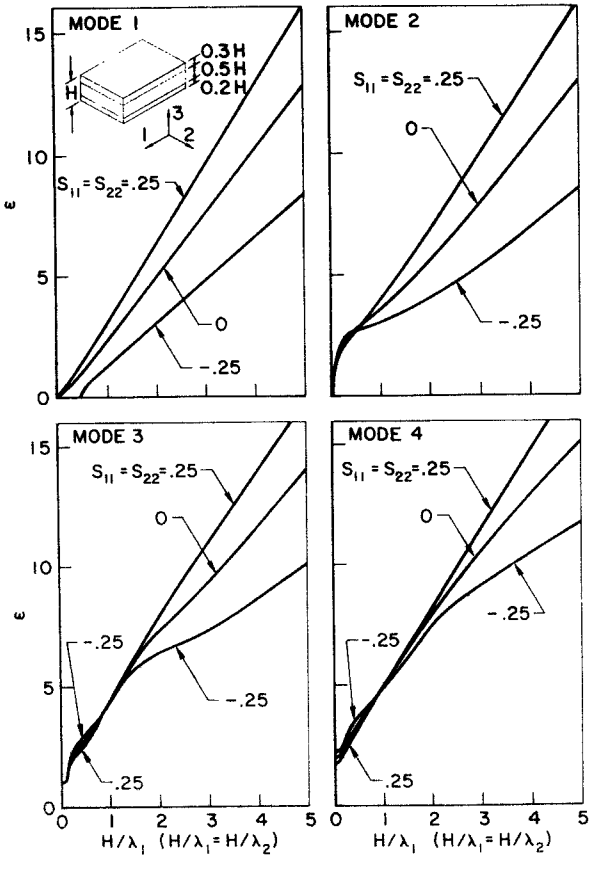

Fig. 4. Frequency spectra for lowest four modes under uniform tension in both x_1 and x_2 directions ($S_{11} = S_{22}$).

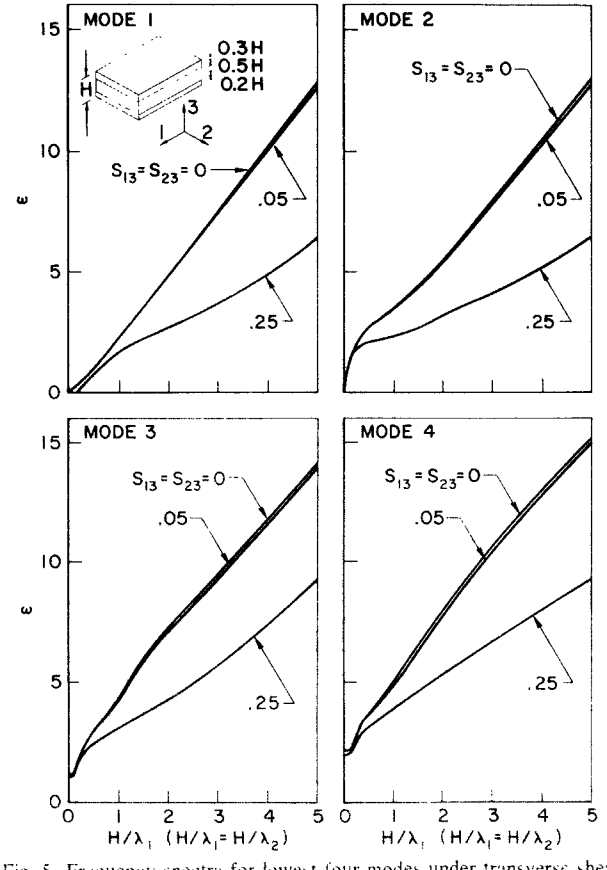

Fig. 5. Frequency spectra for lowest four modes under transverse shearing stress in both directions ($S_{13} = S_{23}$).

controlled prestressing. Frequency analyses of two special cases of prestress on a particular sandwich were carried out in order to illustrate a type of behavior associated with this type of construction.

A plate with cross-sectional construction shown on Fig. 6 was considered. The material properties of the facings are

$$C_{ij} = \begin{bmatrix} 3{\cdot}5 & 1{\cdot}5 & 1{\cdot}5 & & & \\ & 3{\cdot}5 & 1{\cdot}5 & & & \\ & & 3{\cdot}5 & & & \\ \text{Symm.} & & & 1{\cdot}0 & & \\ & & & & 1{\cdot}0 & \\ & & & & & 1{\cdot}0 \end{bmatrix} \quad \text{and } \rho = \pi^2 \tag{27}$$

and that for the core are:

$$C_{ij} = \begin{bmatrix} 0{\cdot}0133 & 0{\cdot}0033 & 0{\cdot}0033 & & & \\ & 0{\cdot}0133 & 0{\cdot}0033 & & & \\ & & 0{\cdot}0133 & & & \\ \text{Symm.} & & & 0{\cdot}005 & & \\ & & & & 0{\cdot}005 & \\ & & & & & 0{\cdot}005 \end{bmatrix} \quad \text{and } \rho = 1{\cdot}0. \tag{28}$$

Only plane wave motions were considered. Stress free surface conditions were prescribed. All initial stresses S_{ij} are normalized with respect to shear modulus G of the facings.

On Fig. 6 are plots of frequency spectra of the lowest four modes for the condition that the faces alone are under a state of uniform extension. On Fig. 7 are plots of frequencies for the lowest four modes for an initial stress state corresponding to pure bending as simulated by uniform tension compression on the two faces. The large differences in the frequencies over the entire range of wave lengths for relatively small changes in the magnitude of the initial stress states suggest that the objective of controlled prestressing to achieve a particular response is highly feasible. Also, it appears to be realistic to achieve this objective without resorting to any unusually complicated or highly imaginative initial stress state.

On Fig. 8 are plots of the displacement and incremental stress distributions through the cross section for the lowest three modes for uniform tension in the faces of the sandwich plate of magnitude $S_{11} = 1{\cdot}0$ for only wave numbers $H/\lambda_1 = 0{\cdot}1$ and $2{\cdot}0$, respectively. It can be seen from these plots that the incremental stress boundary conditions at the free surfaces and the interfaces are met.

On Fig. 9, a comparison is shown of displacement patterns for the lowest mode of the sandwich plate under three different types of prestressing. One is for tension on both faces, another is for compression on both faces and the third depicted a bending condition, and all of these states are associated with $H/\lambda_1 = 2{\cdot}0$ and $S_{11} = 0{\cdot}05$. Most significant to notice is the relative increase in displacement magnitudes in the initially compressed regions.

8. CONCLUDING REMARKS

A solution method has been presented for the vibrational and stability analyses of prestressed laminated orthotropic plates. The formulation and solution method are extensions of earlier investigations of plate and cylinder problems involving no initial stress states. Because of the

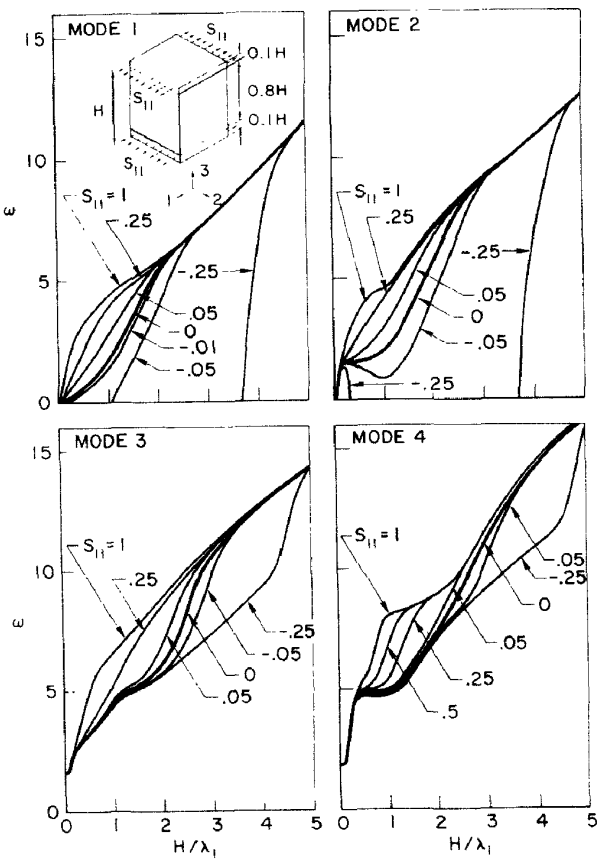

Fig. 6. Frequency-wave number plots of the four lowest modes for the sandwich plate under uniform Tension or compression in the faces.

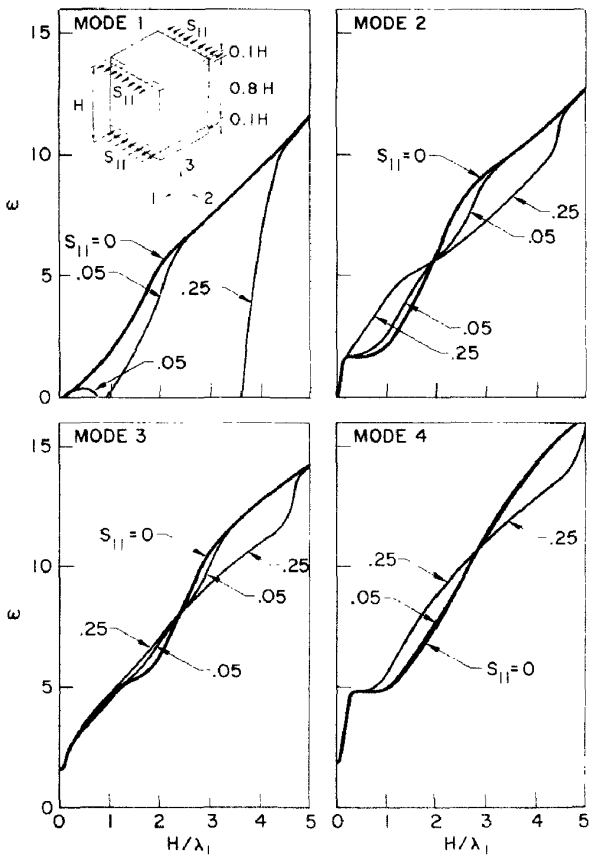

Fig. 7. Frequency-wave number plots of the four lowest modes for the sandwich plate under a bending type initial stress.

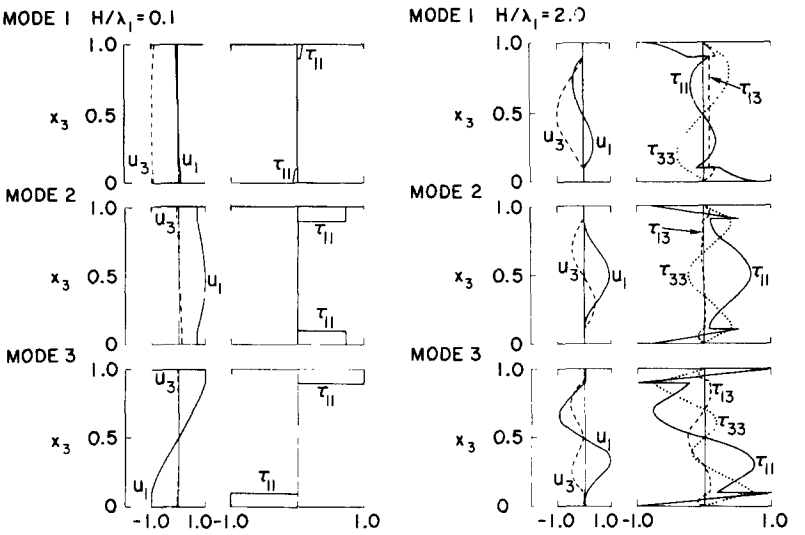

Fig. 8. Displacement and incremental stress distributions in sandwich plate with uniform tension in faces $S_{11} = 1{\cdot}0$ and $H/\lambda_1 = 0{\cdot}1, 2{\cdot}0$.

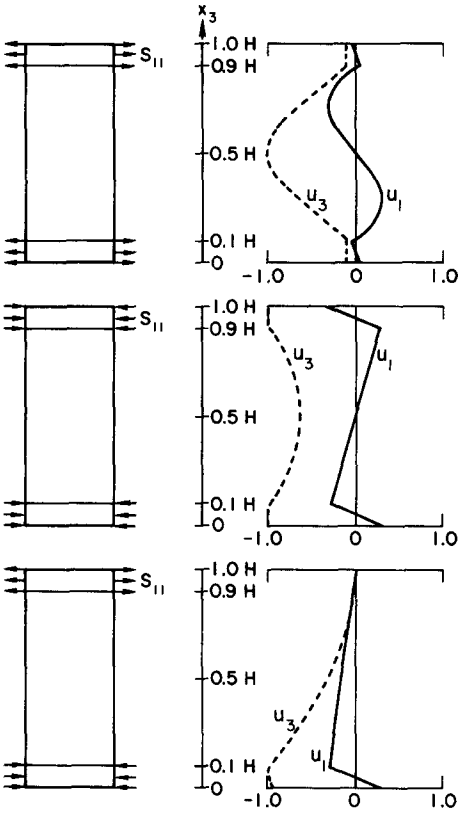

Fig. 9. First mode displacement comparisons for tension, compression, and bending of sandwich plate with $H/\lambda_1 = 2{\cdot}0$ and $S_{11} = 0{\cdot}05$.

computational efficiency and the latitude to incorporate any initial stress state, it is possible to exploit this technique to study a wide variety of plate problems. Several calculations were made on isotropic plates to demonstrate the method's capabilities and lend confidence to its means for extremely accurate solutions over a range of wave numbers. Two additional problems involving composite and sandwich plates were given to further demonstrate the formulation and solution method. It is intended that such a technique will provide the possibility of furthering our insight into the behavior of initially stressed plates in order that residual stress analysis, stability analysis and controlled prestressing may be utilized in the design of plates, especially those of the composite and sandwich types.

REFERENCES

1. A. W. Leissa, *Vibration of Plates*, NASA **SP-160** (1969).
2. S. G. Lekhnitiskii, *Anisotropic Plates*, Gos. Izd. (1957).
3. C. Mei and T. Y. Yang, Free Vibrations of Finite Element Plate Subjected to Complex Middle-Plane Force Systems, *J. Sound and Vibration* **23**, **No. 2**, 145 (1972).
4. G. Herrmann and A. E. Armenàkas, Vibrations and Stability of Plates Under Initial Stress, *J. Engr. Mech. Div. ASCE* **86**, **No. EM5**, 65 (1960).
5. C. T. Sun, On the Equations for Composite Beams Under Initial Stress, *Int. J. Solids Struct.* **8**, 389 (1972).
6. C. T. Sun, Incremental Deformations in Orthotropic Laminated Plates Under Initial Stress, *J. Appl. Mech.* **40**, 193 (1973).
7. M. A. Biot, *Mechanics of Incremental Deformations*. J. Wiley (1965).
8. E. Trefftz, Zur Theorie der Stabilität des elastischen Gleichgewichts, *Z. Angew. Math. Mech.* **13**, 160 (1933).
9. Z. P. Bazant, A Correlation Study of Formulations of Incremental Deformation and Stability of Continuous Bodies, *J. Appl. Mech.* **38**, 919 (1971).
10. S. B. Dong and R. B. Nelson, On Natural Vibrations and Waves in Laminated Orthotropic Plates, *J. Appl. Mech.* **30**, 739 (1972).
11. R. B. Nelson, S. B. Dong and R. D. Kalra, Vibrations and Waves in Laminated Orthotropic Circular Cylinders, *J. Sound Vibration* **18**, 429 (1971).
12. F. K. W. Tso, S. B. Dong and R. B. Nelson, Natural Vibrations of Rectangular Laminated Orthotropic Plates, *Developments in Mechanics* **6**, 891 (1972).
13. S. B. Dong and J. A. Wolf, Jr., Stability Analysis of Structures by a Reduced System of Generalized Coordinates, *Int. J. Solids Struct.* **6**, 1377 (1970).
14. S. B. Dong, J. A. Wolf, Jr. and F. E. Peterson, On a Direct-Iterative Eigensolution Technique, *Int. J. f. Numerical Methods in Engineering* **4**, 155 (1972).
15. J. A. Wolf, Jr. and S. B. Dong, Use of a Reduced System of Generalized Coordinates in a Direct Iterative Eigensolution Technique, *Trans SAE* **80**, **pt. 4**, 2619 (1971).
16. S. P. Timoshenko and J. M. Gere, *Theory of Elastic Stability*, p. 355. McGraw-Hill (1961).

APPENDIX

The non-zero elements of the stiffness and mass matrices appearing in (22) are:

$\mathbf{m}_1$—*matrix* ($m_{ij} = m_{ji}$ symmetric)

$$m_{44} = m_{55} = m_{66} = 4m_{11} = 4m_{22} = 4m_{33} = 4m_{77} = 4m_{88} = 4m_{99}$$
$$= 8m_{14} = 8m_{25} = 8m_{36} = 8m_{47} = 8m_{58} = 8m_{69}$$
$$= -16m_{17} = -16m_{28} = -16m_{39} = 16\rho h/30$$

$\mathbf{k}_1$—*matrix* ($k_{ij} = k_{ji}$ symmetric)

$$k_{11} = k_{77} = 4(C_{11}A + C_{66}B) + 7C_{55}D$$
$$k_{22} = k_{88} = 4(C_{22}B + C_{66}A) + 7C_{44}D$$
$$k_{33} = k_{99} = 4(C_{55}A + C_{44}B) + 7C_{33}D$$
$$k_{44} = 16(C_{11}A + C_{66}B + C_{55}D)$$
$$k_{55} = 16(C_{66}A + C_{22}B + C_{44}D)$$
$$k_{66} = 16(C_{55}A + C_{44}B + C_{33}D)$$
$$4k_{12} = 8k_{15} = -16k_{18} = 8k_{24} = -16k_{27} = k_{45} = 8k_{48} = 8k_{57} = 4k_{78} = 16(C_{12} + C_{66})C$$

$$-k_{13} = k_{79} = 3(C_{13} - C_{55})E$$
$$-k_{23} = k_{89} = 3(C_{23} - C_{44})F$$

$$k_{14} = k_{47} = 2(C_{11}A + C_{66}B) - 8C_{55}D$$
$$k_{16} = -4k_{19} = -k_{34} = 4k_{37} = k_{49} = -k_{67} = 4(C_{13} + C_{55})E$$
$$k_{25} = k_{58} = 2(C_{22}B + C_{66}A) - 8C_{44}D$$
$$k_{26} = -4k_{29} = -k_{35} = 4k_{38} = k_{59} = -k_{68} = 4(C_{23} + C_{44})F$$
$$k_{36} = k_{69} = 2(C_{55}A + C_{44}B) - 8C_{33}D$$
$$k_{17} = -(C_{11}A + C_{66}B) + C_{55}D$$
$$k_{28} = -(C_{22}B + C_{66}A) + C_{44}D$$
$$k_{39} = -(C_{44}B + C_{55}A) + C_{33}D$$

$\mathbf{k}_2$ – *matrix* ($k_{ij} = k_{ji}$ symmetric)

$$k_{11} = k_{77} = B(3S_{22} - S_{11}) + 4S_{12}C + D(21S_{33} - 7S_{11})/4$$
$$k_{22} = k_{88} = A(3S_{11} - S_{22}) + 4S_{12}C + D(21S_{33} - 7S_{22})/4$$
$$k_{33} = k_{99} = A(3S_{11} - S_{33}) + B(3S_{22} - S_{33}) + 6S_{12}C$$
$$k_{44} = 4B(3S_{22} - S_{11}) + 16S_{12}C + 4D(3S_{33} - S_{11})$$
$$k_{55} = 4A(3S_{11} - S_{22}) + 16S_{12}C + 4D(3S_{33} - S_{22})$$
$$k_{66} = 4A(3S_{11} - S_{33}) + 4B(3S_{22} - S_{33}) + 12S_{12}C$$
$$k_{12} = k_{78} = -C(S_{11} + S_{22}) - (8A + 8B + 7D)S_{12}/4$$
$$-4k_{13} = -3k_{16} = 12k_{19} = 3k_{34} = -12k_{37} = -3k_{49} = 3k_{67} = 4k_{79} = 3E(S_{11} + S_{33}) + 3S_{12}F$$
$$-4k_{23} = -3k_{26} = 12k_{29} = 3k_{35} = -12k_{38} = -3k_{69} = 3k_{68} = 4k_{89} = 3F(S_{22} + S_{33}) + 3S_{12}E$$
$$k_{14} = k_{47} = B(3S_{22} - S_{11})/2 + 2S_{12}C + 2D(S_{11} - 3S_{33})$$
$$k_{15} = k_{24} = k_{48} = k_{57} = -C(S_{11} + S_{22})/2 - S_{12}(A + B - 2D)$$
$$k_{25} = k_{58} = A(3S_{11} - S_{22})/2 + 2S_{12}C + 2D(S_{22} - 3S_{33})$$
$$k_{36} = -2k_{39} = k_{69} = A(3S_{11} - S_{33})/2 + B(3S_{22} - S_{33})/2 + 3S_{12}C$$
$$k_{45} = -4C(S_{11} + S_{22}) - 4S_{12}(2A + 2B + D)$$
$$k_{17} = B(S_{11} - 3S_{22})/4 - S_{12}C + D(3S_{33} - S_{11})/4$$
$$k_{18} = k_{27} = C(S_{11} + S_{22})/4 + S_{12}(2A + 2B - D)/4$$
$$k_{28} = A(S_{22} - 3S_{11})/4 - S_{12}C + D(3S_{33} - S_{22})/4$$

$\mathbf{k}_1$ – *matrix*

$$k_{12} = -k_{78} = 3(S_{13}F - S_{23}E)/4 \qquad \text{(antisymmetric, i.e. } k_{ij} = -k_{ji})$$
$$k_{13} = k_{79} = -S_{13}(4A + 2B + 7D)/2 - S_{23}C \qquad \text{(symmetric, i.e. } k_{ij} = k_{ji})$$
$$k_{23} = k_{89} = -S_{13}C - S_{23}(4B + 2A + 7D)/2 \qquad \text{(symmetric)}$$
$$k_{14} = k_{47} = -4k_{17} = 4S_{13}E + 6S_{23}F \qquad \text{(antisymmetric)}$$
$$-k_{15} = 4k_{18} = -k_{24} = 4k_{27} = -k_{48} = -k_{57} = S_{13}F + S_{23}E \qquad \text{(antisymmetric)}$$
$$k_{16} = k_{34} = k_{49} = k_{67} = -S_{13}(2A + B - 8D)/2 - S_{23}C/2 \qquad \text{(symmetric)}$$
$$-k_{25} = 4k_{28} = -k_{58} = -6S_{13}E - 4S_{23}F \qquad \text{(antisymmetric)}$$
$$-k_{36} = 4k_{39} = -k_{69} = 4(S_{13}E + S_{23}F) \qquad \text{(antisymmetric)}$$
$$k_{46} = -4S_{13}(2A + B + 2D) - 4S_{23}C \qquad \text{(symmetric)}$$
$$k_{56} = -4S_{13}C - 4S_{23}(2B + A + 2D) \qquad \text{(symmetric)}$$
$$k_{19} = k_{37} = S_{13}(2A + B - 2D)/4 + S_{23}C/4 \qquad \text{(symmetric)}$$

$$k_{29} = k_{38} = S_{13}C/4 + S_{23}(2B + A - 2D)/4 \quad \text{(symmetric)}$$

$$k_{26} = k_{35} = k_{59} = k_{68} = -S_{13}C/2 - S_{23}(2B + A - 8D)/2 \quad \text{(symmetric)}$$

where

$$A = \xi^2 h/30$$
$$B = \eta^2 h/30$$
$$C = \xi\eta h/30$$
$$D = 1/3h$$
$$E = \xi/6$$
$$F = \eta/6$$
$$\xi = \pi/\lambda_1$$
$$\eta = \pi/\lambda_2$$
$$h = x_{3f} - x_{3b} \text{ (thickness of lamina).}$$

$$C_{11} = C_{11}^{11}$$
$$C_{12} = C_{11}^{22}$$
$$C_{13} = C_{11}^{33}$$
$$C_{22} = C_{22}^{22}$$
$$C_{23} = C_{22}^{33}$$
$$C_{33} = C_{33}^{33}$$
$$C_{44} = C_{33}^{23}$$
$$C_{55} = C_{13}^{13}$$
$$C_{66} = C_{12}^{12}$$